JOC The Journal of Organic Chemistry

Article

pubs.acs.org/joc

Mechanism, Reactivity, and Selectivity in Rh(III)-Catalyzed Phosphoryl-Directed Oxidative C−H Activation/Cyclization: A DFT Study

Liu Liu,[†,‡] Yile Wu,[†] Tao Wang,[†] Xiang Gao,[§] Jun Zhu,*[,∥] and Yufen Zhao*[,†]

[†]Department of Chemistry, College of Chemistry and Chemical Engineering, Key Laboratory for Chemical Biology of Fujian Province, Xiamen University, Xiamen 361005, Fujian, People's Republic of China

[∥]State Key Laboratory of Physical Chemistry of Solid Surfaces and Fujian Provincial Key Laboratory of Theoretical and Computational Chemistry, College of Chemistry and Chemical Engineering, Xiamen University, Xiamen 361005, Fujian, People's Republic of China

[§]School of Pharmaceutical Sciences, Xiamen University, Xiamen 361102, Fujian, People's Republic of China

[‡]Department of Chemistry and Biochemistry, University of California, San Diego, La Jolla, California 92093-0343, United States

Supporting Information

ABSTRACT: Density functional theory calculations (DFT) have been performed on Rh(III)-catalyzed phosphoryl-directed oxidative C−H activation/cyclization to investigate the detailed mechanism, including four basic steps: C−H activation, alkyne insertion, reductive elimination, and catalyst recycling, each of which consists of different steps. Interestingly, the Rh(III)−AgOAc catalyst system was found to be more favorable in the C−H activation step in comparison with the Rh(III)−Ag_2CO_3 system, whereas the Rh(I)−Ag_2CO_3 catalyst system was more efficient for catalyst recycling. Importantly, our calculations suggest that the alkyne insertion process is a reversible step. Reductive elimination is the rate-determining step with an activation energy of 25.0 kcal/mol. In addition, the origin of the reactivity and selectivity difference between diarylacetylenes and dialkylacetylenes or electron-rich and electron-deficient diarylacetylenes was probed by means of comparative DFT calculations. The calculation results show that the electronic effects of alkynes play a key role in the reactivity and selectivity, in line with the experimental observations that diarylacetylenes and electron-rich diarylacetylenes are more reactive than dialkylacetylenes and electron-deficient diarylacetylenes, respectively. Our findings should be useful for further developments of transition-metal-catalyzed C−H activation reactions.

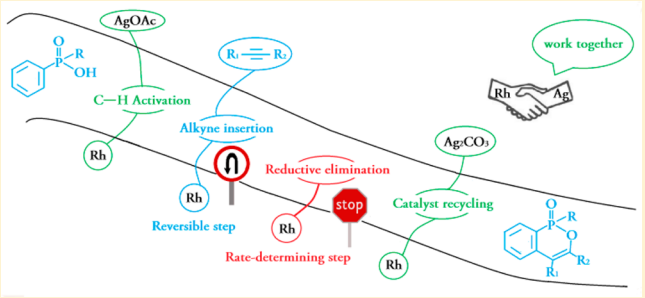

1. INTRODUCTION

The increasing importance of organophosphorus compounds in pharmaceuticals and agrochemicals as well as the use of phosphorus-based ligands has spurred vigorous research into the development of new approaches for the modification of these compounds.[1] The phosphoryl group is one of the most crucial chemical motifs in this area. For example, the presence of a phosphoryl group can significantly improve the metabolic stability and bioavailability of several organic substrates.[2]

Recently, a large number of transition-metal-catalyzed methods for the construction of structurally sophisticated organophosphorus compounds have emerged.[3] Among them, transition-metal-catalyzed phosphoryl-directed C−H functionalization has attracted great attention due to its high efficiency and atom economy.[4] In 2013, Lee and co-workers reported a rhodium(III)-mediated phosphoryl-directed oxidative C−H activation/cyclization with good to excellent yields and broad substrate applicability,[4o,p] undoubtedly providing an exquisite entry to the synthesis of phosphaisocoumarins and phosphorus 2-pyrones that are otherwise difficult to prepare (Scheme 1).[3f]

Considerable recent progress in Rh(III)-mediated C−H functionalization reactions has been accomplished.[5] However, in contrast to a number of experimental[6] and theoretical[7] studies on the mechanisms of palladium(II)-catalyzed C−H activation reactions, the reaction mechanisms of the rhodium-(III)-catalyzed C−H activation have been less studied. Recently

Scheme 1. Rh(III)-Catalyzed Phosphoryl-Directed Oxidative C−H Activation/Cyclization

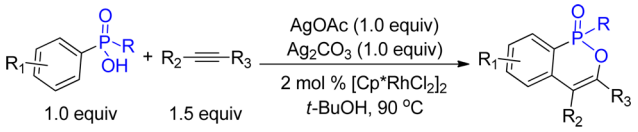

Received: March 17, 2014
Published: May 9, 2014

   dx.doi.org/10.1021/jo500616g | J. Org. Chem. 2014, 79, 5074−5081

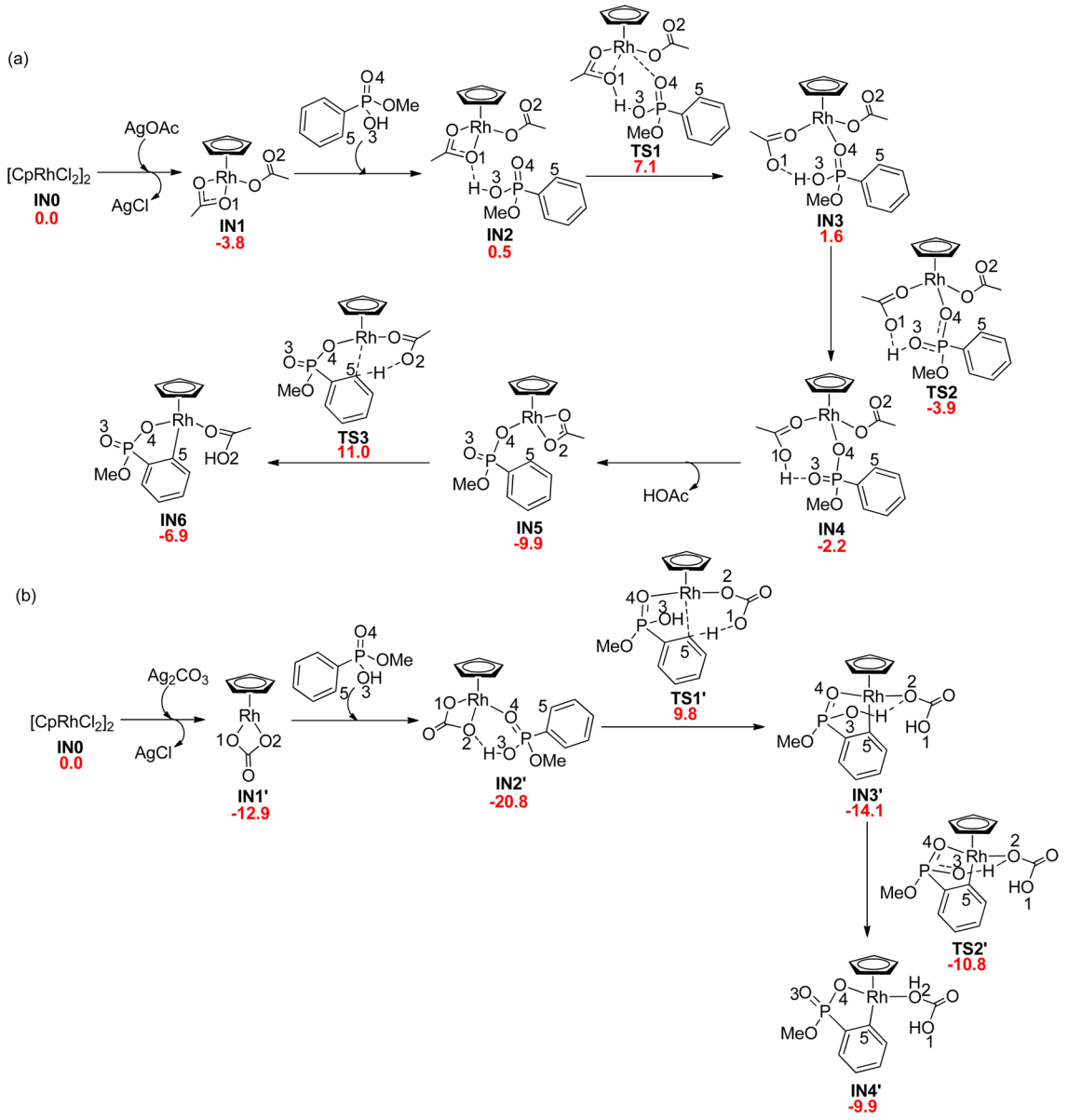

Figure 1. Free energy profiles for the C−H activation step for Rh(III)-catalyzed C−H activation/cyclization. The values are given in kcal/mol.

we found that the hydroxy group of phosphoryl in the palladium(II)-catalyzed ortho olefination can not only protonate the η^1-CH_3COO^- ligand but also stabilize the intermediates and transition states,[7k] which poses an interesting question as to whether the role of the phosphoryl group in Rh(III)-catalyzed phosphoryl-directed oxidative C−H activation/cyclization is similar to that in our previous study. In addition, the different reactivities and selectivities of alkynes and the operating mechanism of the $AgOAc/Ag_2CO_3$ system in these transformations are still not well understood.

Importantly, Rh-catalyzed alkyne insertion into a Rh−C_{sp^2} bond or a Rh−C_{sp^3} bond and reductive elimination of a C−C bond have been broadly studied by several groups.[8] However, to the best of our knowledge, a comparison of Rh(III)-catalyzed alkyne insertions into Rh−X (X = O, C_{sp^2}) bonds has not been studied so far. Here we report theoretical calculations to investigate the detailed reaction mechanism of Rh(III)-catalyzed phosphoryl-directed oxidative C−H activation/cyclization, including four basic steps: C−H activation, alkyne insertion, reductive elimination, and catalyst recycling, each of which consists of different steps, providing hints for further developments of new catalytic reactions.

2. COMPUTATIONAL METHODS

All calculations were carried out with the Gaussian 09 package.[9] Geometry optimizations and frequency calculations were performed with the B3LYP functional.[10] The 6-31G(d)[11] basis set was used for C, H, and O. Rh, Ag, P, Cl, and Br atoms were described by the effective core potentials of Hay and Wadt with a valence double-ζ basis set (LANL2DZ).[12] Polarization functions were added for Rh (ξ_f = 1.35), Ag (ξ_f = 1.611), P (ξ_d = 0.387), Cl (ξ_d = 0.64), and Br (ξ_d = 0.428).[13] Transition states were examined by vibrational analysis and then submitted to intrinsic reaction coordinate (IRC)[14] calculations to determine two corresponding minima. To calculate the single-point electronic energies in solution, the same method with a mixed basis set employing 6-311++G(2d,p)[15] for C, H, O, P, Cl, Br, and SDD[16] for Rh and Ag was used. The default self-consistent reaction field (SCRF) polarizable continuum model (PCM) was used with 2-methyl-2-propanol (dielectric constant ε = 12.47), while Bondi radii[17] were chosen as the atomic radii to define the molecular cavity. The gas-

dx.doi.org/10.1021/jo500616g | J. Org. Chem. 2014, 79, 5074−5081

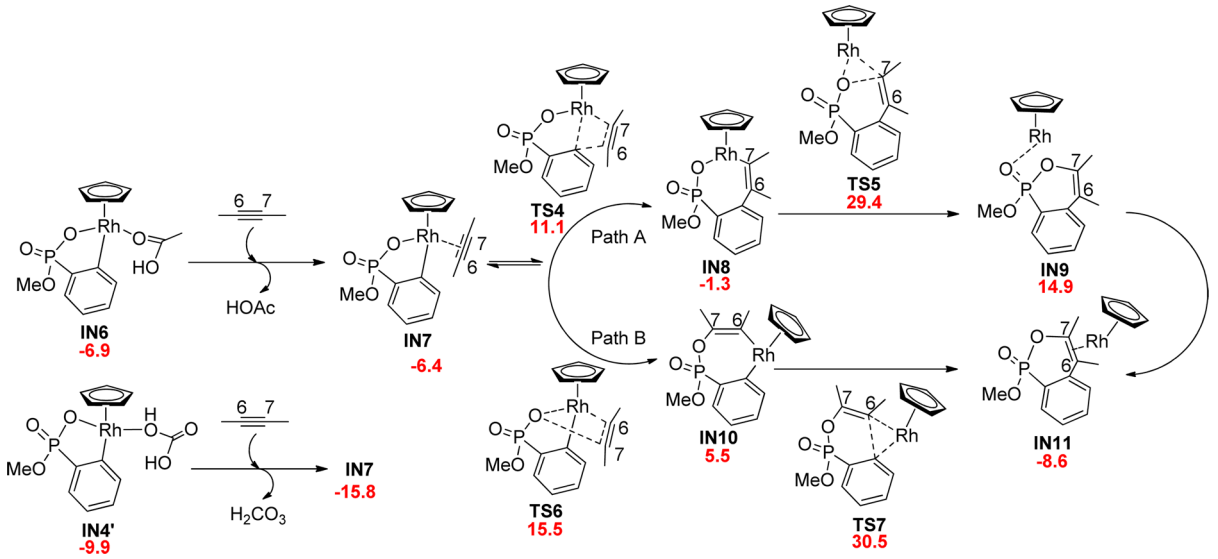

Figure 2. Free energy profile for the alkyne insertion and reductive elimination steps for Rh(III)-catalyzed C−H activation/cyclization. The values are given in kcal/mol.

phase geometry was used for all of the solution-phase calculations. A similar treatment was also used in many recent computational studies.[18] Dispersion correction calculations using the corresponding B3LYP-D functional were performed with the DFT-D3 program of Grimme.[19] The Gibbs energy corrections from frequency calculations and dispersion corrections were added to the single-point energies to obtain the Gibbs free energies in solution. All of the solution-phase free energies reported in the paper correspond to the reference state of 1 mol/L, 298 K.

In the calculations, the model substrates methyl hydrogen phenylphosphonate (PhP(O)(OMe)(OH)), but-2-yne, $[CpRhCl_2]_2$ (Cp = cyclopentadienylanion), and AgOAc were chosen. Relative free energies in solution (2-methyl-2-propanol) were employed to analyze the reaction mechanism. A comparison of some relative free energies of the reaction mechanism obtained with the model substrates (PhP(O)(OMe)(OH) and $[CpRhCl_2]_2$) and the real substrates (PhP(O)(OEt)(OH) and $[Cp^*RhCl_2]_2$ (Cp^* = 1,2,3,4,5-pentamethylcyclopentadienyl anion)) is provided in the Supporting Information. The results showed that the free energies do not differ significantly. For example, the free energies of **TS7** (relative to **IN7**) are 36.9 and 37.4 kcal/mol for the model substrates and the real substrates, respectively. In addition, considering that the B3LYP functional is problematic in treating some transition-metal systems, we evaluated the effects of density functionals in this study. The results show that different DFT methods provide a consistent energy profile (for details see the Supporting Information). Optimized structures were visualized by the CYLview program.[20]

3. RESULTS AND DISCUSSION

3.1. C−H Bond Activation. On the basis of the kinetic study[21] of a sodium acetate promoted $[Cp^*RhCl_2]_2$-catalyzed C−H activation reaction, the plausible active catalytic species has been assumed to be the coordinatively unsaturated $[Cp^*Rh(OAc)]^+$, where the rhodium center would be easily attacked by nucleophilic reagents. In addition, ligand-assisted concerted metalation−deprotonation was found to be the most favorable process in the Pd-[7b,l] and Ir-catalyzed[22] C−H activation steps. It is important to note that, in the experimental study,[4o,p] both AgOAc (1.0 equiv) and Ag_2CO_3 (1.0 equiv) were needed under the optimized reaction conditions (Scheme 1). Therefore, as shown in Figure 1, two active catalyst complexes (**IN1** and **IN1′**) could be considered as the starting points for the C−H activation steps, which are generated from the catalyst precursor $[Cp^*RhCl_2]_2$ in the presence of AgOAc and Ag_2CO_3, respectively.

Figure 1a depicts the CH_3COO^- ligand promoted C−H bond activation step. Initially, the approach of the substrate PhP(O)(OMe)(OH) toward **IN1** (−3.8 kcal/mol) generates the complex **IN2** (0.5 kcal/mol) by the intermolecular hydrogen bond O3−H···O1. Since the oxygen of P═O is more nucleophilic than those of P−OH and P−OMe,[7k,23] subsequently, O4 coordinates to the Rh center via the six-membered transition state **TS1** (7.1 kcal/mol) with an activation energy of 10.9 kcal/mol relative to **IN1**. Then, the intermediate **IN3** (1.6 kcal/mol) is formed, which bears the intramolecular hydrogen bond O3−H···O1, promoting an intramolecular hydrogen transfer through the transition state **TS2** (−3.9 kcal/mol) to generate the new intermediate **IN4** (−2.2 kcal/mol) with a stabilizing O3···H−O1 bond. From **IN4**, the more stable intermediate **IN5** (−9.9 kcal/mol), bearing one η^2-CH_3COO^- in the ligand field, could be located via the removal of the neutral acetic acid. Finally, a CH_3COO^--assisted concerted metalation−deprotonation process takes place via the six-membered transition state **TS3** (the activation barrier is 20.9 kcal/mol), leading to the formation of the intermediate **IN6** (−6.9 kcal/mol), which is feathered by a Rh-containing five-membered-ring structure.

On the other hand, the CO_3^{2-} ligand can also facilitate the C−H bond activation step.[7a,24] Thus, we also turn our attention to this step (Figure 1b). In **IN1′**, the Rh center is coordinatively unsaturated; therefore, the substrate PhP(O)(OMe)(OH) can readily bind to **IN1′**, forming the very stable intermediate **IN2′** (−20.8 kcal/mol) with the intramolecular hydrogen bond O3−H···O2. Subsequent CO_3^{2-} ligand mediated C−H bond activation occurs with an activation energy of 30.6 kcal/mol. Then a proton transfer from O3 to O2 occurs with an activation barrier of 3.3 kcal/mol. The role of the hydroxy group of phosphoryl is to stabilize the intermediates and transition states and also to act as a proton donor so that the CH_3COO^- and HCO_3^- ligands could be protonated to generate the corresponding neutral acids for easy removal, which is found to be similar to our previous report.[7k]

dx.doi.org/10.1021/jo500616g | J. Org. Chem. 2014, 79, 5074−5081

Our calculations reveal that the first role of the AgOAc/Ag_2CO_3 system is to provide sources of CH_3COO^- and CO_3^{2-} ligands to facilitate the C−H activation process. Note that the neutral HOAc and H_2CO_3 could be readily replaced by alkynes in **IN6** and **IN4′**, respectively, giving the same product **IN7** (Figure 2). Moreover, the activation energy (rate-determining step) of the CH_3COO^- ligand mediated C−H activation process is computed to be 20.9 kcal/mol, which is 9.7 kcal/mol lower than that of the CO_3^{2-}-mediated process, indicating AgOAc-mediated C−H bond activation is more favorable. Thus, **IN6** was chosen for the further study.

3.2. Alkyne Insertion and Reductive Elimination. The alkyne insertion step (Figure 2) begins with the removal of the neutral acetic acid from **IN6** to create a vacant coordination site on the Rh(III) center and allow the coordination of the C≡C triple bond of but-2-yne, generating **IN7** with a energy of −6.4 kcal/mol. From **IN7**, two pathways are considered (Figure 2, paths A and B): the but-2-yne may insert into the Rh−C_{sp^2} bond (path A) via **TS4** (11.1 kcal/mol) to form **IN8** (−1.3 kcal/mol), in which the C6−C7 double bond is conjugated with the phenyl π bond, or insert into the Rh−O bond (Path B) via **TS6** (15.5 kcal/mol) to form **IN10** (5.5 kcal/mol).

The highest occupied molecular orbital (HOMO) of **IN7** (Figure 3) is mainly localized at the π orbital of the phenyl ring.

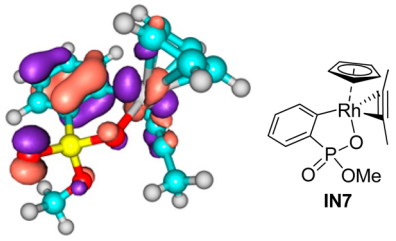

Figure 3. HOMO (isovalue = 0.05) of **IN7**.

Thus, alkyne attacks at the C_{sp^2} could lead to favorable orbital overlap between the phenyl π orbital and the alkyne π^* orbital. Therefore, the activation energy of **TS4** (18.0 kcal/mol, relative to **IN6**) is 4.4 kcal/mol lower than that (22.4 kcal/mol, relative to **IN6**) of **TS6**. The free energy of **IN8** is 6.8 kcal/mol lower than that of **IN10**. Interestingly, the relative free energies of **IN8** (−1.3 kcal/mol) and **IN10** (5.5 kcal/mol) are 5.1 and 11.9 kcal/mol higher than that of **IN7** (−6.4 kcal/mol), respectively, indicating that both alkyne insertion processes are reversible and the two intermediates **IN8** and **IN10** are in equilibrium with each other.

Subsequent reductive elimination processes may take place from both **IN8** and **IN10**, via C−O (**TS5**, 29.4 kcal/mol) and C−C bond formation (**TS7**, 30.5 kcal/mol), leading to the cyclization products **IN9** (14.9 kcal/mol) and **IN11** (−8.6 kcal/mol), respectively. The activation energy of the C−O bond reductive elimination is 30.7 kcal/mol, which is 5.7 kcal/mol higher than that of the C−C bond reductive elimination. In addition, the π complex **IN11** is much more stable than the σ complex **IN9** by 23.5 kcal/mol, clearly demonstrating that path B is more favorable than path A.

In summary, although the alkyne insertion into Rh−C_{sp^2} bond is energetically favorable, the next C−O bond reductive elimination is too energy demanding. Furthermore, the process of the alkyne insertion into Rh−C_{sp^2} bond is found to be reversible so that the resting state **IN8** could regenerate **IN7**, which could undergo Rh−O insertion. Therefore, the preferred alkyne insertion step involves two key steps: alkyne insertion into the Rh−O bond and C−C bond reductive elimination.

3.3. Reactivity and Selectivity of Different Alkynes. It is interesting to note that the reactivities and selectivities of alkynes were found to be much different in the alkyne competition experiments (Scheme 2).[4o,p] For example, a competition experiment between diphenylacetylene and 5-decyne (1.5 equiv each) generates mainly the phosphaisocoumarin **1a** (Scheme 2, top equation). A mixture of electron-rich (*p*-methoxy) and electron-deficient (*p*-bromo) diarylacetylenes was treated with phenylphosphonic acid monoester to generate phosphaisocoumarin **2a** as the major product (Scheme 2, bottom equation), which was obtained from the electron-rich alkyne.

On the basis of these experimental observations, we performed comparative DFT calculations to identify key factors that control the reactivities and selectivities. As shown in Table 1, the relative free energies among the four alkynes in the alkyne insertion step are influenced by several factors. Notably, the activation energies (**IN6** → **TS6**) of diarylacetylenes are much lower than that of dialkylacetylene (Table 1, entries 1 and 2), which could mainly be attributed to electronic effects. For example, the energy of the HOMO in 1,2-diphenylethyne is 0.03 eV higher than that in but-2-yne so that 1,2-diphenylethyne is more nucleophilic (Table 1, entries 1 and 2). The energy of the LUMO in but-2-yne is computed to be 0.68 eV, whereas that in 1,2-diphenylethyne is −0.05 eV, indicating 1,2-diphenylethyne is a better candidate for enhancing back-donation from the metal center.

Figure 4 illustrates the structures of the four transition states. The O−C7 bond length (2.145 Å) in **TS6B** is much shorter

Scheme 2. Alkyne Competition Experiments

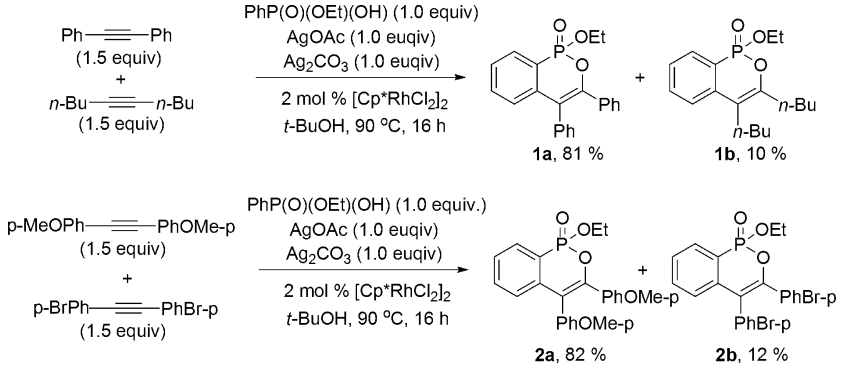

dx.doi.org/10.1021/jo500616g | J. Org. Chem. 2014, 79, 5074−5081

Table 1. Comparative Studies of the Different Reactivities in Various Alkynes by DFT Calculations

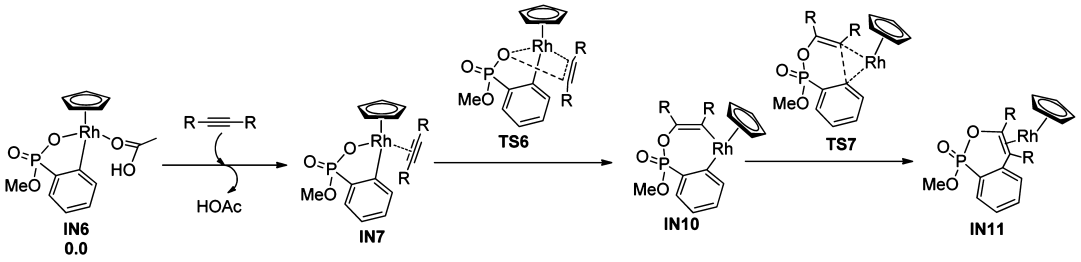

				ΔG^b					
entry	R in alkyne	E(HOMO)^a	E(LUMO)^a	IN7	TS6	IN10	TS7	IN11	$\Delta\Delta G^c$
1	Ph	−0.21	−0.05	1.4	18.8	7.8	32.8	−0.6	25.0
2	Me	−0.24	0.68	0.5	22.4	12.4	37.4	−1.7	25.0
3	*p*-MeOPh	−0.19	−0.03	1.8	17.4	8.4	32.5	−2.7	24.1
4	*p*-BrPh	−0.22	−0.06	1.2	18.4	7.4	33.8	−1.4	26.4

^{a}The HOMOs and LUMOs of alkynes are calculated in the gas phase at the B3LYP/6-31G(d)+LanL2DZ level. The values are given in eV. ^{b}The values are given in kcal/mol. ^{c}The activation energies (**IN10** → **TS7**) are given in kcal/mol.

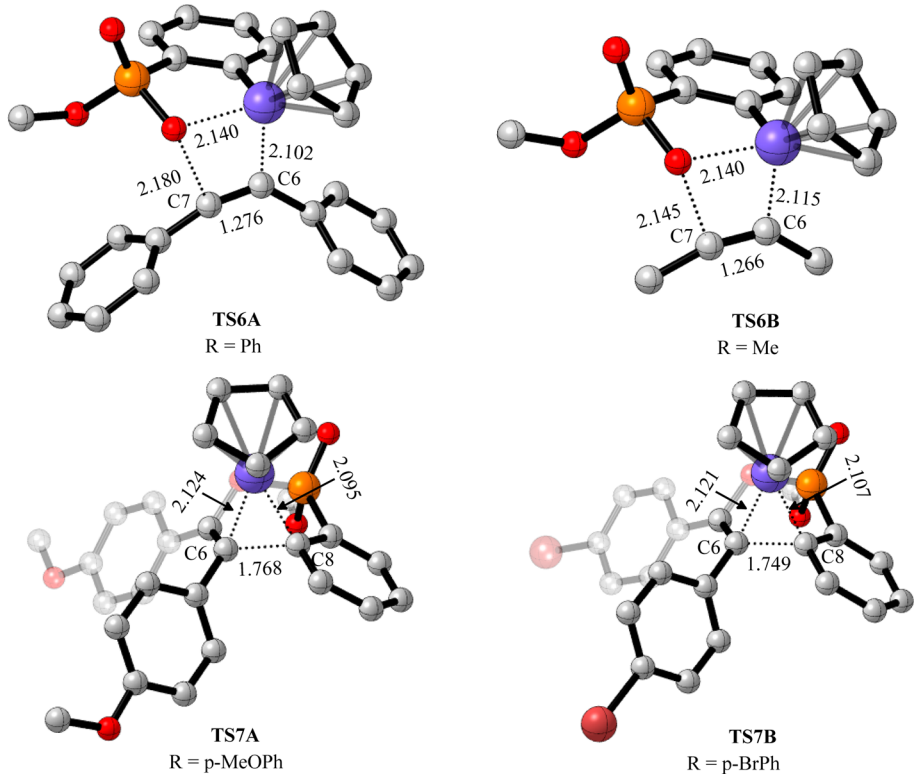

Figure 4. Structures (Å) of four transition states. Hydrogen atoms are omitted for clarity.

than that (2.180 Å) in **TS6A**, indicating that but-2-yne requires more energy to insert into the Rh−O bond. Thus, diarylacetylenes are more reactive than dialkylacetylenes, in line with the experimental observations (Scheme 2, top equation). Similarly, the C6−C8 bond length is 1.768 Å in **TS7A**, which is longer than that (1.749 Å) in **TS7B**. Consequently, the activation energy of **TS7B** (relative to the corresponding resting state) is 1.3 kcal/mol higher than that of **TS7A**, which could be one of the key factors in controlling the reactivities and selectivities between electron-deficient and electron-rich diarylacetylenes.

3.4. Catalyst Recycling. Apparently, the formal oxidation state of the metal center in **IN11** is Rh(I). We then focus on the Ag(I) salt promoted oxidation process. Because the Ag atom has a single electron, it may easily build up to the Ag cluster. Furthermore, experimental measurements show that the Ag−Ag bond is quite strong (38.3 kcal/mol).[25] Therefore, the recovery of the Rh(III) catalyst may start when a AgOAc or a Ag_2CO_3 molecule approaches **IN11**, forming the intermediate **IN12** (−24.5 kcal/mol) or **IN12′** (−26.6 kcal/mol) (Figure 5), respectively. Separation of the product from **IN12** or **IN12′** is thermodynamically feasible, since these processes are exergonic by 20.7 or 3.6 kcal/mol, respectively.

Although **IN13** is more stable than **IN13′** by 15.0 kcal/mol, subsequent Ag−Ag bond formation in **TS8** (very late transition state, activation energy 22.6 kcal/mol) is much more energy demanding than that in **TS8′** (very early transition state, activation energy 0.9 kcal/mol), definitely showing that the

dx.doi.org/10.1021/jo500616g | J. Org. Chem. 2014, 79, 5074−5081

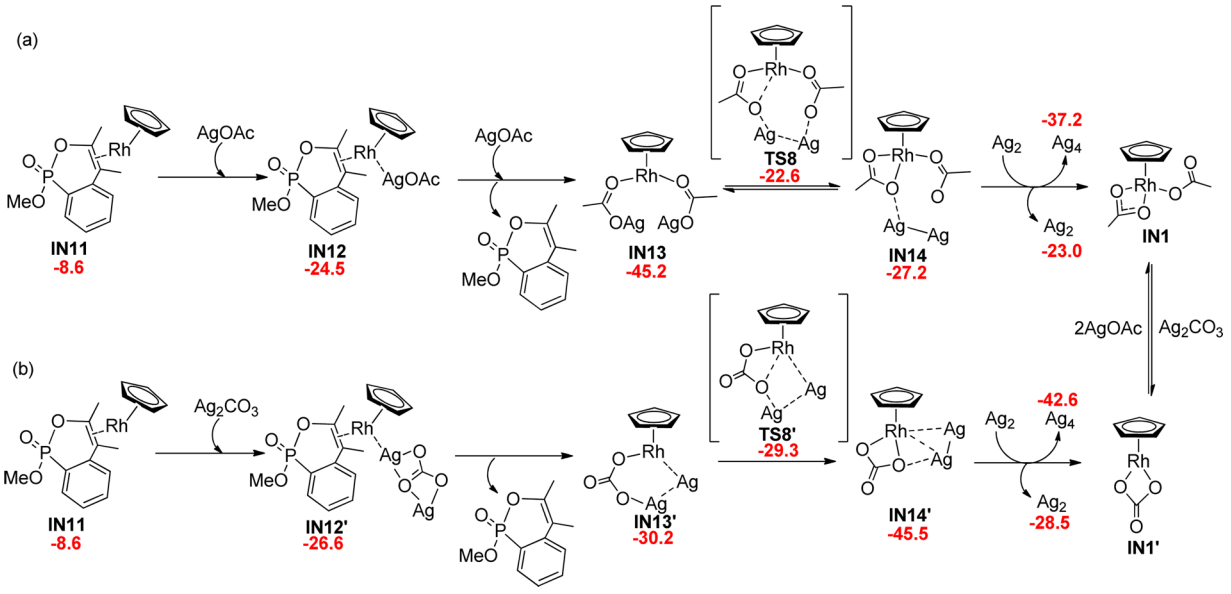

Figure 5. Free energy profile for the catalyst recycling step for Rh(III)-catalyzed C−H activation/cyclization. The values are given in kcal/mol.

AgOAc-mediated Ag−Ag bond formation step is reversible, whereas the Ag_2CO_3-mediated step is irreversible. However, as the Ag_2 concentrates, it can build up,[26] promoting a forward shift in the chemical equilibrium. Thus, the second role of the AgOAc/Ag_2CO_3 system is to recycle the Rh(III) catalyst.

4. CONCLUSIONS

We have investigated the detailed mechanism and origin of reactivity and selectivity of different alkynes in Rh(III)-catalyzed phosphoryl-directed oxidative C−H activation/cyclization, including four basic steps: C−H activation, alkyne insertion, reductive elimination, and catalyst recycling. The activation energies in all possible pathways were computed. In the C−H activation step, the preferred catalytic cycle was facilitated by the Rh−AgOAc catalyst system. The activation energy (rate-determining step) is computed to be 20.9 kcal/mol, which is 9.7 kcal/mol lower than that for the Rh−Ag_2CO_3 catalyst system. In the alkyne insertion and reductive elimination steps, two pathways were considered: alkyne insertion into the Rh−C_{sp^2} bond followed by C−O bond formation or alkyne insertion into the Rh−O bond and consequent C−C bond formation. Interestingly, both processes of alkyne insertion into the Rh−C_{sp^2} and Rh−O bond are computed to be reversible. However, the C−O bond reductive elimination is too energy demanding, indicating that the preferred alkyne insertion step should take place when an alkyne inserts into the Rh−O bond followed by C−C bond reductive elimination. The C−C bond formation is the rate-determining step with an activation energy of 25.0 kcal/mol. Comparative DFT calculations were carried out to identify key factors that control the reactivities and selectivities of different alkynes. The results suggest that electronic effects play a key role. In the catalyst recycling step, Ag_2CO_3 is more efficient than AgOAc in regenerating the active catalytic Rh(III) complex. Our findings can serve as a benchmark for other similar Rh(III)-catalyzed reactions, which might open a new avenue to the design of more efficient C−H activation reactions.

■ ASSOCIATED CONTENT

Ⓢ Supporting Information

Text, tables, and figures giving the complete ref 9, effects of different density functionals, effects of the real substrates and the model substrates, a comparison of the different P-bonded oxygen atoms attacking the Rh center, 3D optimized structures, energies of intermediates and transition states, Cartesian coordinates for the optimized structures and the first frequency from calculations. This material is available free of charge via the Internet at http://pubs.acs.org.

■ AUTHOR INFORMATION

Corresponding Authors

*J.Z.: e-mail, jun.zhu@xmu.edu.cn; web, http://junzhu.chem8.org.

*Y.Z.: e-mail, yfzhao@xmu.edu.cn; web, http://chem.xmu.edu.cn/group/yfzhao/zhao-home.html.

Notes

The authors declare no competing financial interest.

■ ACKNOWLEDGMENTS

We acknowledge financial support from the National Basic Research Program of China (2012CB821600, 2013CB910700, and 2011CB808504), the Chinese National Natural Science Foundation (21305115, 21232005, 21103142, and 21172184), the Program for New Century Excellent Talents in University (NCET-13-0511), the Program for Changjiang Scholars and Innovative Research Team in University and the Fundamental Research Funds for the Central Universities (2012121021). Thanks are also given to the China Scholarship Council for a Graduate Fellowship (L.L.).

■ REFERENCES

(1) Selected recent reviews: (a) Montchamp, J.-L. *Acc. Chem. Res.* **2014**, *47*, 77−87. (b) Xu, Q.; Zhou, Y.-B.; Zhao, C.-Q.; Yin, S.-F.; Han, L.-B. *Mini-Rev. Med. Chem.* **2013**, *13*, 824−835. (c) Skarżyńska, A. *Coord. Chem. Rev.* **2013**, *257*, 1039−1048.

(2) Selected recent reviews: (a) Queffélec, C.; Petit, M.; Janvier, P.; Knight, D. A.; Bujoli, B. *Chem. Rev.* **2012**, *112*, 3777−3807. (b) Demmer, C. S.; Krogsgaard-Larsen, N.; Bunch, L. *Chem. Rev.*

dx.doi.org/10.1021/jo500616g | *J. Org. Chem.* 2014, 79, 5074−5081

2011, *111*, 7981−8006. (c) Van der Jeught, S.; Stevens, C. V. *Chem. Rev.* **2009**, *109*, 2672−2702.

(3) Selected recent publications: (a) Feng, C.-G.; Ye, M.; Xiao, K.-J.; Li, S.; Yu, J.-Q. *J. Am. Chem. Soc.* **2013**, *135*, 9322−9325. (b) Liu, L.; Wang, Y.; Zeng, Z.; Xu, P.; Gao, Y.; Yin, Y.; Zhao, Y. *Adv. Synth. Catal.* **2013**, *355*, 659−666. (c) Wang, T.; Sang, S.; Liu, L.; Qiao, H.; Gao, Y.; Zhao, Y. *J. Org. Chem.* **2014**, *79*, 608−617. (d) Li, X.; Yang, F.; Wu, Y.; Wu, Y. *Org. Lett.* **2014**, *16*, 992−995. (e) Chen, S.-Y.; Zeng, R.-S.; Zou, J.-P.; Asekun, O. T. *J. Org. Chem.* **2014**, *79*, 1449−1453. (f) Mo, J.; Kang, D.; Eom, D.; Kim, S. H.; Lee, P. H. *Org. Lett.* **2013**, *15*, 26−29. (g) Xu, J.; Zhang, P.; Gao, Y.; Chen, Y.; Tang, G.; Zhao, Y. *J. Org. Chem.* **2013**, *78*, 8176−8183. (h) Jouvin, K.; Veillard, R.; Theunissen, C.; Alayrac, C.; Gaumont, A.-C.; Evano, G. *Org. Lett.* **2013**, *15*, 4592−4595. (i) Wang, Y.; Gan, J.; Liu, L.; Yuan, H.; Gao, Y.; Liu, Y.; Zhao, Y. *J. Org. Chem.* **2014**, *79*, 3678−3683.

(4) For Pd-catalyzed phosphoryl-directed C−H functionalization reactions, see: (a) Zhang, H.-Y.; Yi, H.-M.; Wang, G.-W.; Yang, B.; Yang, S.-D. *Org. Lett.* **2013**, *15*, 6186−6189. (b) Chan, L. Y.; Cheong, L.; Kim, S. *Org. Lett.* **2013**, *15*, 2186−2189. (c) Meng, X.; Kim, S. *J. Org. Chem.* **2013**, *78*, 11247−11254. (d) Kang, D.; Cho, J.; Lee, P. H. *Chem. Commun.* **2013**, *49*, 10501−10503. (e) Eom, D.; Jeong, Y.; Kim, Y. R.; Lee, E.; Choi, W.; Lee, P. H. *Org. Lett.* **2013**, *15*, 5210−5213. (f) Guan, J.; Wu, G.-J.; Han, F.-S. *Chem. Eur. J.* **2014**, *20*, 3301−3305. (g) Zhang, H.; Hu, R.-B.; Zhang, X.-Y.; Li, S.; Yang, S.-D. *Chem. Commun.* **2014**, *50*, 4686−4689. (h) Ma, Y.-N.; Tian, Q.-P.; Zhang, H.-Y.; Zhou, A.-X.; Yang, S.-D. *Org. Chem. Front.* **2014**, *1*, 284−288. (i) Hu, R.-B.; Zhang, H.; Zhang, X.-Y.; Yang, S.-D. *Chem. Commun.* **2014**, *50*, 2193−2195. For Ru-catalyzed phosphoryl-directed C−H functionalization reactions, see: (j) Park, Y.; Jeon, I.; Shin, S.; Min, J.; Lee, P. H. *J. Org. Chem.* **2013**, *78*, 10209−10220. For Rh-catalyzed phosphoryl-directed C−H functionalization reactions, see: (k) Itoh, M.; Hashimoto, Y.; Hirano, K.; Satoh, T.; Miura, M. *J. Org. Chem.* **2013**, *78*, 8098−8104. For Rh-catalyzed phosphoryl-directed C−H functionalization reactions, see: (l) Park, S.; Seo, B.; Shin, S.; Son, J.-Y.; Lee, P. H. *Chem. Commun.* **2013**, *49*, 8671−8673. (m) Zhao, D.; Nimphius, C.; Lindale, M.; Glorius, F. *Org. Lett.* **2013**, *15*, 4504−4507. (n) Mo, J.; Lim, S.; Park, S.; Ryu, T.; Kim, S.; Lee, P. H. *RSC Adv.* **2013**, *3*, 18296−18299. (o) Park, Y.; Seo, J.; Park, S.; Yoo, E. J.; Lee, P. H. *Chem. Eur. J.* **2013**, *19*, 16461−16468. (p) Seo, J.; Park, Y.; Jeon, I.; Ryu, T.; Park, S.; Lee, P. H. *Org. Lett.* **2013**, *15*, 3358−3361. (q) Unoh, Y.; Hashimoto, Y.; Takeda, D.; Hirano, K.; Satoh, T.; Miura, M. *Org. Lett.* **2013**, *15*, 3258−3261.

(5) Selected recent publications: (a) Chan, W.-W.; Lo, S.-F.; Zhou, Z.; Yu, W.-Y. *J. Am. Chem. Soc.* **2012**, *134*, 13565−13568. (b) Li, Y.; Xue, D.; Lu, W.; Wang, C.; Liu, Z.-T.; Xiao, J. *Org. Lett.* **2014**, *16*, 66−69. (c) Neely, J. M.; Rovis, T. *J. Am. Chem. Soc.* **2013**, *135*, 66−69. (d) Neely, J. M.; Rovis, T. *J. Am. Chem. Soc.* **2014**, *136*, 2735−2738. (e) Yu, S.; Li, X. *Org. Lett.* **2014**, *16*, 1220−1223. (f) Feng, C.; Loh, T.-P. *Angew. Chem., Int. Ed.* **2014**, *53*, 2722−2726. (g) Gong, B.; Shi, J.; Wang, X.; Yan, Y.; Li, Q.; Meng, Y.; Xu, H. E.; Yi, W. *Adv. Synth. Catal.* **2014**, *356*, 137−143. (h) Shi, Z.; Boultadakis-Arapinis, M.; Koester, D. C.; Glorius, F. *Chem. Commun.* **2014**, *50*, 2650−2652.

(6) Selected recent publications: (a) Giri, R.; Maugel, N.; Li, J.-J.; Wang, D.-H.; Breazzano, S. P.; Saunders, L. B.; Yu, J.-Q. *J. Am. Chem. Soc.* **2007**, *129*, 3510−3511. (b) Baxter, R. D.; Sale, D.; Engle, K. M.; Yu, J.-Q.; Blackmond, D. G. *J. Am. Chem. Soc.* **2012**, *134*, 4600−4606. (c) Engle, K. M.; Wang, D.-H.; Yu, J.-Q. *J. Am. Chem. Soc.* **2010**, *132*, 14137−14151. (d) Giri, R.; Yu, J.-Q. *J. Am. Chem. Soc.* **2008**, *130*, 14082−14083. (e) Lyons, T. W.; Sanford, M. S. *Chem. Rev.* **2010**, *110*, 1147−1169. (f) Ma, S.; Villa, G.; Thuy-Boun, P. S.; Homs, A.; Yu, J.-Q. *Angew. Chem., Int. Ed.* **2014**, *53*, 734−737. (g) Engle, K. M.; Mei, T.-S.; Wasa, M.; Yu, J.-Q. *Acc. Chem. Res.* **2012**, *45*, 788−802. (h) Chai, D. I.; Thansandote, P.; Lautens, M. *Chem. Eur. J.* **2011**, *17*, 8175−8188.

(7) Selected recent publications: (a) Boutadla, Y.; Davies, D. L.; Macgregor, S. A.; Poblador-Bahamonde, A. I. *Dalton Trans.* **2009**, 5820−5831. (b) Yang, Y.-F.; Cheng, G.-J.; Liu, P.; Leow, D.; Sun, T.-Y.; Chen, P.; Zhang, X.; Yu, J.-Q.; Wu, Y.-D.; Houk, K. N. *J. Am. Chem. Soc.* **2014**, *136*, 344−355. (c) Zhang, L.; Fang, D.-C. *J. Org. Chem.* **2013**, *78*, 2405−2412. (d) Yang, X.; Hall, M. B. *J. Phys. Chem. A* **2009**, *113*, 2152−2157. (e) Clot, E.; Eisenstein, O.; Jasim, N.; Macgregor, S. A.; McGrady, J. E.; Perutz, R. N. *Acc. Chem. Res.* **2011**, *44*, 333−348. (f) Cheng, G.-J.; Yang, Y.-F.; Liu, P.; Chen, P.; Sun, T.-Y.; Li, G.; Zhang, X.; Houk, K. N.; Yu, J.-Q.; Wu, Y.-D. *J. Am. Chem. Soc.* **2014**, *136*, 894−897. (g) Pascual, S.; de Mendoza, P.; Braga, A. A. C.; Maseras, F.; Echavarren, A. M. *Tetrahedron* **2008**, *64*, 6021−6029. (h) Balcells, D.; Clot, E.; Eisenstein, O. *Chem. Rev.* **2010**, *110*, 749−823. (i) Lian, B.; Zhang, L.; Chass, G. A.; Fang, D.-C. *J. Org. Chem.* **2013**, *78*, 8376−8385. (j) Giri, R.; Lan, Y.; Liu, P.; Houk, K. N.; Yu, J.-Q. *J. Am. Chem. Soc.* **2012**, *134*, 14118−14126. (k) Liu, L.; Yuan, H.; Fu, T.; Wang, T.; Gao, X.; Zeng, Z.; Zhu, J.; Zhao, Y. *J. Org. Chem.* **2014**, *79*, 80−87. (l) Davies, D. L.; Donald, S. M. A.; Macgregor, S. A. *J. Am. Chem. Soc.* **2005**, *127*, 13754−13755.

(8) Selected recent publications: (a) Wang, Y.; Wang, J.; Su, J.; Huang, F.; Jiao, L.; Liang, Y.; Yang, D.; Zhang, S.; Wender, P. A.; Yu, Z.-X. *J. Am. Chem. Soc.* **2007**, *129*, 10060−10061. (b) Yu, Z.-X.; Cheong, P. H. -Y.; Liu, P.; Legault, C. Y.; Wender, P. A.; Houk, K. N. *J. Am. Chem. Soc.* **2008**, *130*, 2378−2379. (c) Xu, X.; Liu, P.; Lesser, A.; Sirois, L. E.; Wender, P. A.; Houk, K. N. *J. Am. Chem. Soc.* **2012**, *134*, 11012−11025. (d) Xu, X.; Liu, P.; Shu, X.-Z.; Tang, W.; Houk, K. N. *J. Am. Chem. Soc.* **2013**, *135*, 9271−9274. (e) Liu, P.; Sirois, L. E.; Cheong, P. H.-Y.; Yu, Z.-X.; Hartung, I. V.; Rieck, H.; Wender, P. A.; Houk, K. N. *J. Am. Chem. Soc.* **2010**, *132*, 10127−10135.

(9) Frisch, M. J.; et al. *Gaussian 09, Revision B.01*; Gaussian, Inc., Wallingford, CT, 2010.

(10) (a) Lee, C.; Yang, W.; Parr, R. G. *Phys. Rev. B* **1988**, *37*, 785−789. (b) Stephens, P. J.; Devlin, F. J.; Chabalowski, C. F.; Frisch, M. J. *J. Phys. Chem.* **1994**, *98*, 11623−11627.

(11) (a) Ditchfield, R.; Hehre, W. J.; Pople, J. A. *J. Chem. Phys.* **1971**, *54*, 724−728. (b) Hehre, W. J.; Ditchfield, R.; Pople, J. A. *J. Chem. Phys.* **1972**, *56*, 2257−2261. (c) Hariharan, P. C.; Pople, J. A. *Theor. Chim. Acta* **1973**, *28*, 213−222. (d) Dill, J. D.; Pople, J. A. *J. Chem. Phys.* **1975**, *62*, 2921−2923. (e) Francl, M. M.; Pietro, W. J.; Hehre, W. J.; Binkley, J. S.; Gordon, M. S.; DeFrees, D. J.; Pople, J. A. *J. Chem. Phys.* **1982**, *77*, 3654−3665.

(12) Wadt, W. R.; Hay, P. J. *J. Chem. Phys.* **1985**, *82*, 284−298.

(13) (a) Höllwarth, A.; Böhme, M.; Dapprich, S.; Ehlers, A. W.; Gobbi, A.; Jonas, V.; Kohler, K. F.; Stegmann, R.; Veldkamp, A.; Frenking, G. *Chem. Phys. Lett.* **1993**, *208*, 237−240. (b) Ehlers, A.; Böhme, M.; Dapprich, S.; Gobbi, A.; Höllwarth, A.; Jonas, V.; Köhler, K.; Stegmann, R.; Veldkamp, A.; Frenking, G. *Chem. Phys. Lett.* **1993**, *208*, 111−114.

(14) (a) Fukui, K. *J. Phys. Chem.* **1970**, *74*, 4161−4163. (b) Fukui, K. *Acc. Chem. Res.* **1981**, *14*, 363−368.

(15) (a) Krishan, R.; Binkley, J. S.; Seeger, R.; Pople, J. A. *J. Chem. Phys.* **1980**, *72*, 650−654. (b) McLean, A. D.; Chandler, G. S. *J. Chem. Phys.* **1980**, *72*, 5639−5648. (c) Clark, T.; Chandrasekhar, J.; Spitznagel, G. W.; Schleyer, P. v. R. *J. Comput. Chem.* **1983**, *4*, 294−301.

(16) Andrae, D.; Haeussermann, U.; Dolg, M.; Stoll, H.; Preuss, H. *Theor. Chim. Acta* **1990**, *77*, 123−141.

(17) Bondi, A. *J. Phys. Chem.* **1964**, *68*, 441−451.

(18) Selected recent publications: (a) Park, S. H.; Kwak, J.; Shin, K.; Ryu, J.; Park, Y.; Chang, S. *J. Am. Chem. Soc.* **2014**, *136*, 2492−2502. (b) Vidhani, D. V.; Krafft, M. E.; Alabugin, I. V. *J. Org. Chem.* **2014**, *79*, 352−364. (c) Zhang, X.; Ke, Z.; DeYonker, N. J.; Xu, H.; Li, Z.-F.; Xu, X.; Zhang, X.; Su, C.-Y.; Phillips, D. L.; Zhao, C. *J. Org. Chem.* **2013**, *78*, 12460−12468. (d) Liu, L.; Zhang, S.; Chen, H.; Lv, Y.; Zhu, J.; Zhao, Y. *Chem.—Asian J.* **2013**, *8*, 2592−2595. (e) Yu, Z.; Lan, Y. *J. Org. Chem.* **2013**, *78*, 11501−11507.

(19) (a) Grimme, S.; Antony, J.; Ehrlich, S.; Krieg, H. *J. Chem. Phys.* **2010**, *132*, 154104. (b) Grimme, S. *J. Comput. Chem.* **2006**, *27*, 1787−1799. (c) Grimme, S. *J. Comput. Chem.* **2004**, *25*, 1463−1473.

(20) Legault, C. Y. *CYLview, 1.0b*; Université de Sherbrooke, Sherbrooke, Québec, Canada, 2009; www.cylview.org.

(21) Li, L.; Brennessel, W. W.; Jones, W. D. *Organometallics* **2009**, *28*, 3492−3500.

(22) Davies, D. L.; Donald, S. M. A.; Al-Duaij, O.; Macgregor, S. A.; Pölleth, M. *J. Am. Chem. Soc.* **2006**, *128*, 4210−4211.
(23) A comparison of the different P-bonded oxygen atom attacks at the Rh center is provided in the Supporting Information.
(24) García-Cuadrado, D.; de Mendoza, P.; Braga, A. A. C.; Maseras, F.; Echavarren, A. M. *J. Am. Chem. Soc.* **2007**, *129*, 6880−6886.
(25) Huber, K. P.; Herzberg, G. *Molecular Spectra and Molecular Structure I*; Van Nostrand Reinhold: New York, 1950.
(26) Silver mirror was observed after the reaction.